IEEE Access
Multidisciplinary | Rapid Review | Open Access Journal

Received December 26, 2018, accepted January 18, 2019, date of publication January 31, 2019, date of current version February 20, 2019.

Digital Object Identifier 10.1109/ACCESS.2019.2896622

Nondestructive Measurement of Conformal Coating Thickness on Printed Circuit Board With Ultra-High Resolution Optical Coherence Tomography

XIAO SHAO[1], XINJIAN CHEN[1], XIAOJUN YU[2], YA HU[3], LINBO LIU[4], FEI SHI[1], WEI SHAO[5], AND JIANHUA MO[1]

[1]School of Electronics and Information Engineering, Soochow University, Suzhou 215006, China
[2]School of Automation, Northwestern Polytechnical University, Xi'an 710072, China
[3]Engineering Development Department, Automotive Electronics Unit, Bosch Automotive Products (Suzhou) Co., Ltd., Suzhou 215021, China
[4]School of Electrical and Electronic Engineering, Nanyang Technological University, Singapore 639798
[5]Department of Electrical and Computer Engineering, The University of Iowa, Iowa City, IA 52242, USA

Corresponding author: Jianhua Mo (joshuamo@gmail.com)

This work was supported in part by the National Natural Science Foundation of China under Grant 61705184 and Grant 81401451, in part by the Natural Science Foundation of the Jiangsu Province under Grant BK20140365, in part by the Natural Science Basic Research Plan in Shaanxi Province of China under Grant 2018JQ6014, in part by the Fundamental Research Funds for the Central Universities under Grant G2018KY0308, in part by the National Research Foundation Singapore under Grant NRF-CRP13-2014-05, in part by the Ministry of Education Singapore under Grant MOE2013-T2-2-107, in part by the National Medical Research Council Singapore under Grant NMRC/CBRG/0036/2013, in part by the Biomedical Research Council, A*STAR, Singapore, under Grant H17/01/a0/008, and in part by the NTU-AIT-MUV Program in Advanced Biomedical Imaging under Grant NAM/15005.

ABSTRACT Conformal coating (CC) is widely used to protect printed circuit board from corrosion, mold growth, and electrical failures. To ensure effective protection, the thickness of the CC layer needs to be well controlled. However, to date, the coating thickness is usually measured in a destructive way under microscopes. In this paper, we proposed to use optical coherence tomography (OCT) to measure the CC thickness nondestructively. Specifically, to obtain a good accuracy in thickness measurement, we constructed a spectral domain OCT with the ultra-high axial resolution to image the CC layer in three dimensions and developed an image segmentation algorithm to detect the CC layer from the OCT images. Finally, we evaluated the effectiveness of the proposed method by comparing it with the conventional method, and the results demonstrate that the measurement by our method is consistent with that by the microscope. This also indicates that OCT with high axial resolution can potentially be used to measure the CC thickness accurately and nondestructively.

INDEX TERMS Optical coherence tomography, conformal coating, thickness measurement, image segmentation.

I. INTRODUCTION

Conformal coating (CC) is a thin transparent layer with thickness of tens to hundreds micrometers, which is usually made of synthetic resin or plastic, applied on top of printed circuit boards (PCBs) [1], [2]. It serves to protect PCBs from environmental, electrical, mechanical and chemical effects, such as moisture, dust, mechanical stress, thermal stress, corrosion, solvents, chemical vapors and so on. Consequently, CC has been widely used to increase the reliability and lifetime of PCBs, especially in automotive, avionics and military electronics [1]. For example, CC has proven to be an effective way to mitigate tin whisker to prevent arcing and short circuits. It has also been found that CC could prevent deep corrosion on nickel-palladium-gold-finished terminals [3]. To ensure an effective protection, the thickness of the conformal coating has been considered to be one of the key properties, and needs to be well controlled during the curing process and measured after the curing process is completed [4].

The CC thickness can be measured either non-destructively or destructively. One simple non-destructive way is to measure directly with micrometer, which however requires a

The associate editor coordinating the review of this manuscript and approving it for publication was Kin Kee Chow.

measurement on uncoated PCB as a base. Beta-backscatter method is another non-destructive way, yet careful calibration is required [5]. As for destructive measurement, the common way is to cut the PCB and measure the thickness of the coating from its cross-section under a microscope [6]. This method can only be carried out based on sampling inspection due to its destructive nature; and it is also time-consuming and suffers from the intra-operator variation. In addition to those disadvantages mentioned above, both non-destructive and destructive measurement methods are only suited practically for point-measurement rather than area-scanning. In industrial practice, however, area-scanning is needed to evaluate the coverage uniformity of the conformal coating, determining the protection efficacy [3], [4].

Optical coherence tomography (OCT) is a low-coherence optical interferometric imaging technique and can provide three-dimensional image of scattering medium non-destructively [7]. The axial resolution of OCT imaging is decoupled from the transverse resolution; and therefore, OCT is ideal for both layered structure imaging and layer thickness measurement, for example, its initial targeted application, retinal imaging [7], [8]. Till now, OCT has been successfully applied in ophthalmic imaging as a clinical routine tool and also exhibited a great potential in other clinical areas, such as dermatology, cardiology, gastroenterology and so on [9]–[11]. In recent years, great efforts have also been devoted to applying OCT to nondestructive inspection in industry, in particular, to measure the thickness of various industrial materials and products, such as automotive paints, egg shell and multi-layered foils [12]–[14], and the profile of the surface and internal interface [15]. In addition, OCT has also been used for inspecting jade, silicon integrated-circuits, industrial ceramics, LEDs and so on [16]–[20]. In particular for printed electronics products, OCT has been employed to evaluate the internal and surface structure of RF antenna and the encapsulation quality of organic field effect transistor [21], [22]. However, these works employed time domain OCT setups, which is too slow (Axial line rate: <1000 Hz) and the axial scanning range is too short ($\leq$ 300μm) to meet the inspection speed requirements. In addition, the femtosecond light source and the free space optics are very costly and complicated which precludes its industrial applications. Recently, Fourier-domain OCT has been introduced to monitor the structural properties of screen printed interdigitated electrodes in roll-to-roll process [20]. Although the imaging speed was improved by more than 100 times, the axial resolution of 4 μm is not enough for measuring the CC thickness accurately.

In this study, we specially designed a spectral-domain OCT system, which provides ultra-high depth resolution to ensure a high accuracy in thickness measurement, and also exhibits advantages of lower-cost, being more flexible and robust to facilitate industrial applications as compared to time-domain OCT. Furthermore, we developed an image segmentation algorithm to detect and measure the thickness of the CC layer from OCT images, which is more robust than the previous reported amplitude-based method [22]. We verified experimentally that the proposed SD-OCT and algorithm is an advanced tool for measuring the thickness of the PCB conformal coating.

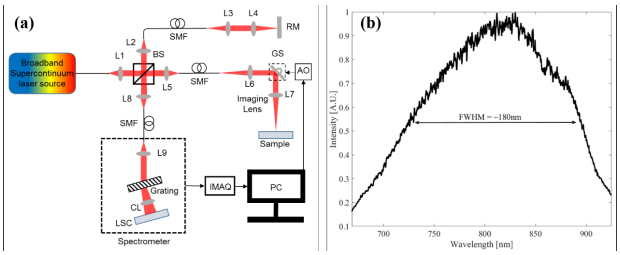

FIGURE 1. (a) Schematic of ultra-high resolution OCT system constructed. SMF: single mode fiber; L1-L9: achromatic lens; PC: personal computer; BS: beam splitter; RM: reference mirror; IMAQ: image acquisition; GS: galvo scanner; AO: analog output; CL: camera lens; LSC: line scan camera. (b) The laser output spectrum detected by the line-scan CCD array in the system.

II. METHODS

A. ULTRA-HIGH RESOLUTION OPTICAL COHERENCE TOMOGRAPHY

To accurately measure the thickness of the PCB conformal coating, a fiber-optic ultra-high resolution OCT system as shown in Fig. 1(a) was constructed in house for imaging. A free space beam-splitter could help the influence of the limited spectral response of the fiber-couplers. We used single mode fibers to deliver the sample and the reference light so that the system can achieve a modular construction for more flexible and robust operation. We chose a low-cost supercontinuum light source (SC-5, Yangtze Soton Laser, Wuhan, CHN) to meet the budget requirement of industrial applications. It has a center wavelength of 810 nm and a spectral bandwidth of 180 nm at full width at half maximum (FWHM) as shown in Fig. 1(b). In the experiments, the light output power was measured to be 15.6 mW with the repetition rate and the power ratio set to be 5 MHz and 30%, respectively. The laser output was directed to a non-polarizing cubic 50:50 broadband beam-splitter (BS008, Thorlabs Inc., Newtown, NJ, USA) by a collimation lens L1 (AC050-010-B-ML, Thorlabs Inc., Newtown, NJ, USA) and a single mode fiber (630-HP, Thorlabs Inc., Newtown, NJ, USA). The beam was then split and directed into the reference arm and sample arm optics. While the reference arm consists of a lens L2 (AC050-010-B-ML, Thorlabs Inc., Newtown, NJ, USA), a single mode fiber (630-HP, Thorlabs Inc., Newtown, NJ, USA), a lens L3 (AC050-015-B-ML, Thorlabs Inc., Newtown, NJ, USA), an objective L4 (M Plan Apo NIR 20×-, Edmund Optics Inc., Barrington, NJ, USA) and a reference mirror, the sample arm optics followed the same path length as the reference arm, with the collimation lens L6 (identical to L3) and the objective lens L7 (identical to L4) for sample scanning.

The light reflected back from both arms was finally recombined by the beam splitter, and directed to the same type

of single mode fiber (630-HP, Thorlabs Inc., Newtown, NJ, USA). The generated interference signals were eventually coupled into a spectrometer by a collimation lens L8 (AC050-010-B-ML, Thorlabs Inc., Newtown, NJ, USA). The optics (lens and fibers) in the sample and reference arms were specially chosen to be identical to minimize the dispersion. Tele-centric scanning system with two galvo scanners (GVSM002/M, Thorlabs Inc., Newtown, NJ, USA) was designed in the sample arm. The illumination power on the sample was measured to be 5.63 mW in the experiments. To compensate the dispersion effects caused by the fiber length difference between the two-arm optics, the method proposed in [23] was adopted for system calibration.

The spectrometer mentioned above was constructed with a collimation lens L9 (AC127-030-B-ML, Thorlabs, Newtown, NJ, USA), a diffraction grating (1200 l/mm @ 830nm, Wasatch Photonics, Logan, UT, USA), a camera lens (AF Nikkor 85mm f/1.8D, Nikon, Tokyo, JPN), and a line scan CCD array with 2048 pixels (AViiVA EM4, E2V, Chelmsford, ENG). The detected signal was transferred to a workstation through a camera link cable and an image acquisition card (KBN-PCE-CL4-F, Bitflow, Woburn, MA, USA) with a 12-bit digitization resolution. In our experiments, both the camera and the galvo scanners were synchronized by a triggering signal generated by the workstation. The effective camera detection range covered by the laser spectrum at FWHM was measured to be 1467 pixels. The spectrometer efficiency η, which is the ratio of the CCD detected energy per pixel to the incident energy per pixel as described by Eq. (1), was measured by blocking the sample arm optics while illuminating a reference light onto the spectrometer.

$$\eta = \frac{F_{wd} \times Q_e}{S_{pr} \times \left((P_{ref} \times \tau / N_{op})/P_s\right) \times (F_{wd}/2^{b_t})} \quad (1)$$

where F_{wd}, Q_e, S_{pr}, τ, P_s and b_t are full-well depth, quantum efficiency, spectral response, exposure time, pixel size and bit depth of the camera, respectively. With the reference power P_{ref} set to be 5.31 μW, the spectrometer efficiency η was measured to be 0.421 in this study.

B. ULTRA-HIGH RESOLUTION OCT SYSTEM CHARACTERIZATION

The ultra-high resolution OCT system performance is characterized by its spatial resolution in the transverse and axial directions, respectively. To determine the lateral resolution of the system, an *en-face* image of a 1951 USAF resolution chart was extracted from an acquired 3D volumetric image. As shown in Fig. 2(a), Group 7 element 1 is the smallest pattern distinguishable, corresponding to a resolution of 7.8 μm (line pair width). While to measure the system axial resolution, we inserted an actuated iris diaphragm (SM05D5, Thorlabs Inc., Newtown, NJ, USA) with a total attenuation of 34.5 dB into the sample arm optics, and measured an A-line profile by placing a BK7 prism (with an attenuation of 14 dB) at the focal plane of the sample arm optics. As shown in Fig. 2(b), the axial resolution was measured to be $\sim$ 1.72 μm in air.

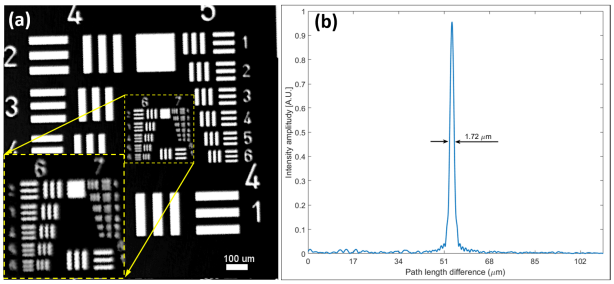

FIGURE 2. The performance characterization of ultra-high resolution OCT. (a) Group 7 element 1 is the smallest pattern distinguishable, corresponding to a resolution of 7.8 μm (line pair width). (b) System axial resolution is measured to be 1.72 μm in air at a path length difference of 55 μm.

Furthermore, we also calculated the ratio of the A-line peak power to its root mean square value, and estimated the signal-to-noise ratio (SNR) to be 47.4 dB at a path length difference of $\sim$ 95 μm. Hence, the ultra-high resolution OCT system overall sensitivity was estimated to be $\sim$95.9 dB.

C. SIGNAL PROCESSING

1) OCT SIGNAL PROCESSING AND IMAGE RECONSTRUCTION

In a spectrometer based OCT, the interferogram is sampled in the detector pixel space (n-space with n being the index of the detector pixels) other than uniform k-space. As a result, the sampled intereferogram needs to be remapped before being inversely Fourier-transformed to generate the depth-profile. In this paper, we employed an effective calibration method to remap the n-space 'chirped' interferograms to k-space perfect sinusoids. Such a calibration method is based on the idea that when a single reflector is used as the sample, OCT should generate a perfect sinusoidal interferogram in k-space, and thus a mapping vector could be found to remap the n-space 'chirped' interferograms. Specifically, the proposed calibration method consists of two main steps: firstly, two interferograms were recorded at different path lengths and subsequently a remapping vector was extracted via Hilbert transform, and then the k-space interferogram was obtained via linear interpolation; secondly, linear regression was employed to implement the dispersion compensation process to obtain the desired k-space interferograms.

Once the k-space interferograms were obtained, OCT signals were fast Fourier transformed to generate the cross-sectional OCT images (B-scans). These cross-sectional images were also combined together to reconstruct the 3D images, and *en-face* images at different depths can be extracted by z-direction projection. Five adjacent original cross-sectional images were averaged to alleviate the influences of noise prior to implementing the coating thickness measurement algorithm.

2) COATING THICKNESS MEASUREMENT ALGORITHM

PCB is usually constructed with multiple layers and the layer underneath the conformal coating is the solder mask layer as

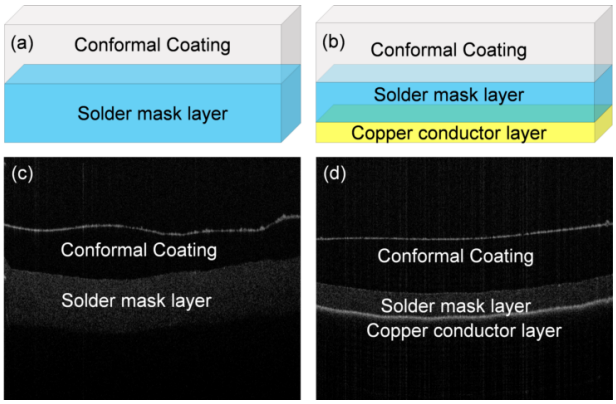

FIGURE 3. Illustration of PCB superficial layer structures: (a) schematic of two layer structure; (b) schematic of three layer structure. (c) and (d) are the corresponding OCT B-scans of (a) and (b), respectively.

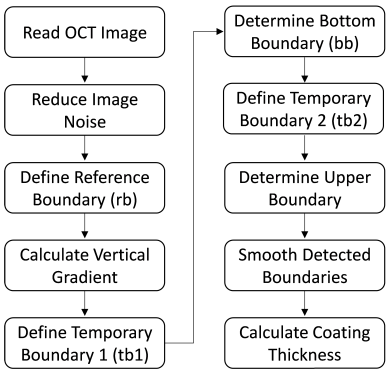

FIGURE 4. Flow chart of the coating thickness measurement algorithm implementation on single B-scan.

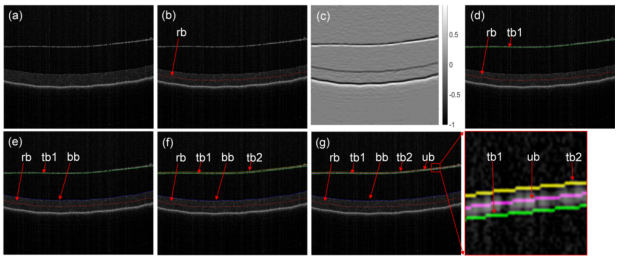

FIGURE 5. The intermediate results from the thickness measurement algorithm implementation: (a) Original B-scan of PCB; (b) Original B-scan overlaid with the reference boundary (rb) denoted with red line; (c) Vertical gradient image; (d) B-scan in Fig. 5(b) overlaid with the first temporary boundary (tb1) denoted with green line; (e) B-scan in Fig. 5(d) overlaid with the bottom boundary (bb) denoted with blue line; (f) B-scan in Fig. 5(e) overlaid with the second temporary boundary (tb2) denoted with yellow line; (g) B-scan in Fig. 5(f) overlaid with the upper boundary (ub) denoted with pink line.

shown in Figs. 3(a)-(b). In certain regions of the PCB, there also exists a copper conductor layer (Fig. 3(b)). These two or three layers described above are the depth region which can be imaged by OCT due to the limited penetration of the light as shown in Figs. 3(c)-(d). It is observed that the imaging depth in the region without a copper conductor layer is deeper (Fig. 3(c)) than that with a copper conductor layer (Fig. 3(d)). This can be accounted for by both the strong reflections at the interface between the solder mask layer and the copper conductor layer, and the large attenuation property of the copper conductor layer. It is also found that the conformal coating layer shows two distinct boundaries, resulting from the refractive index discontinuities between the conformal coating layer and its neighboring layers. This allows for developing the coating thickness measurement algorithm based on the image gradient.

The algorithm implementation is illustrated by the flow chart in Fig. 4 with the intermediate results shown in Fig. 5, and each step is described in detail as follows,

step 1 Read an OCT B-scan that is averaged over 5-adjacent original B-scans (Fig. 5(a)) and then apply a median filter and a Gaussian filter to further reduce the noise.

step 2 To facilitate the detection of the coating layer's boundaries, an artificial boundary called reference boundary (rb) is generated. Each column of the image is convoluted with a 50-by-1 mean filter, and then those pixels with the maximal intensity in each column are connected into a line, which is subsequently smoothed with a Savitzky-Golay filter to generate the reference boundary. The reference boundary is always located in the solder mask layer above the copper foil layer as denoted with a red line in Fig. 5(b).

step 3 A 10-by-1 vertical gradient is calculated on each column of the image according to the equation below:

$$G_{i,j} = \sum_{k=i+1}^{k=i+5} INT_{k,j} - \sum_{k=i-5}^{k=i-1} INT_{k,j} \qquad (2)$$

where G is the vertical gradient, INT is the intensity image, i and k represent the pixel's row index, j represents the column index of the pixel. The gradient image is depicted in Fig. 5(c).

step 4 Take the maximal gradient in the depth region above the reference boundary to define a temporary boundary (tb1). Next, the bottom boundary (bb) of the conformal coating layer can be found by searching the pixels with the minimal gradient in the depth region between tb1 and rb in each column. The process of finding tb1 and bb is illustrated by Fig. 5(d)-5(e), wherein the tb1 and bb are denoted with green and blue lines, respectively.

step 5 Take the minimal gradient in the depth region above tb1 to define another temporary boundary (tb2) as denoted with yellow line in Fig. 5(f). The middle line between tb1 and tb2 is considered to be the upper boundary of the coating layer (pink line in Fig. 5(g)).

step 6 Both the detected upper boundary and bottom boundary above are smoothed by a Savitzky-Golay filter and then for each column, the thickness is obtained by measuring the axial gap between the upper boundary and the bottom boundary.

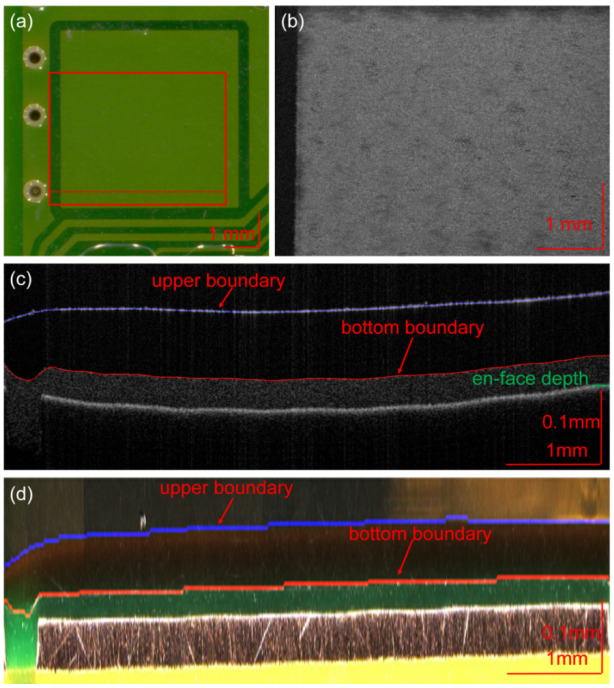

FIGURE 6. (a) Photograph of the PCB, (b) OCT en-face image yielded through averaging over the imaging depth from about 39 to 42 μm below the bottom boundary of the coating layer, corresponding to the area denoted with the red rectangle in Fig. 6(a); Boundary detection of the conformal coating layer on: (c) Ultra-high resolution OCT B-scan, (d) Microscopic cross-sectional image.

step 7 Repeat the procedures above on each B-scan to generate the two-dimensional thickness map.

It is worth noting that, to obtain the actual physical thickness, the thickness calculated with the algorithm needs to be scaled with the reciprocal of the conformal coating's group index. The group index of the conformal coating is experimentally determined to be 1.408 using the method reported in [24].

III. RESULTS AND DISCUSSION

In this study, a PCB with conformal coating was chosen for evaluating our method. The PCB was coated with the CC on the basis of modified polyurethane resins (PETERS, ELPEGUARD SL 1301 ECO = FLZ, Peters, Kempen, DEU). In the curing process, the conformal coating was sprayed onto the PCB first, and then underwent a two-step curing process, ultraviolet curing followed by oven curing, which was customized by the PCB manufacturer from the standard protocol provided by the coating manufacturer (the detailed curing protocol cannot be disclosed due to the technical confidentiality required by the PCB manufacturer). Figure 6(a) shows the photograph of the PCB with the conformal coating and the rectangle delineated with red solid line indicates the region scanned by the ultra-high resolution OCT. The *en-face* view of the OCT image is shown in Fig. 6(b), appearing to match well with the photograph discussed above.

Figure 6(c) shows a typical OCT B-scan acquired along the dashed line in Fig. 6(a). The corresponding microscopic cross-sectional image (Fig. 6(d)) is identified by registering one plating through hole in the microscopic image with the same one in the OCT B-scan. It is clearly seen that the region imaged includes both two-layer structure and three-layer structure as described in Sec. 2.3.2. The two-layer structure is present in a narrow region on the left end of the image, corresponding to the dark green part in Fig. 6(a). The microscopic cross-sectional view of this region in Fig. 6(d) confirms that this two-layer structure comprises a coating layer seated on top of the solder mask layer. The remaining part of the image appears to be three-layer structured, corresponding to the light green part in Fig. 6(a). The strong reflection by the third layer implies that this can be the copper foil layer, which was further confirmed by the cross-sectional image in Fig. 6(d). In addition, the coating layer is almost transparent in the OCT image, however, its refractive index mismatches with the air and the solder mask layer, resulting in two bright edges, which were utilized to segment the coating layer for the thickness measurement. The upper and bottom boundaries of the coating layer generated by our segmentation algorithm are delineated with blue and red lines overlaid on the B-scan (Fig. 6(c)). Obviously, the blue and red lines match well with the top and bottom boundaries, indicating a fairly good accuracy of our thickness measurement method. The axial distance of the two boundaries in the B-scan can be translated into the real physical thickness by scaling it with the reciprocal of the coating group index ($n = 1.408$).

To further assess the accuracy of the proposed thickness measurement method, the PCB was sent to one third party to measure the coating thickness in the conventional way after it was imaged by ultra-high resolution OCT. The PCB was cut to get its cross-section exposed under a microscope, which consequently destroyed the PCB permanently. Thus, only one cross-section of the PCB was photographed under microscope as shown in Fig. 6(d). It is clearly seen that the microscopic image showed a very consistent structure as the B-scan in Fig. 6(c). The copper layer generated a very strong reflection again, which is similar to the findings in the B-scan. The thickness measurement on the microscopic image was achieved by manually segmenting the coating layer. The segmentation result was represented by the blue and red lines overlaid on the microscopic image. The coating layer thickness is just equivalent to the vertical gap of the two lines above.

Figure 7 presents the comparison of the coating layer thickness measured by the two different methods discussed above. Overall, these two methods show a good agreement in the thickness measurement over a range of about 5 mm. The inconsistency was assessed by calculating the difference between the results obtained with the two measurement methods as illustrated in Fig. 7(b). The difference varied from -4.28 to 2.54 μm, and exhibited an averaged difference of -0.82 μm with a standard deviation of 1.30 μm. Fig. 7(c) is the histogram of the thickness difference distribution in

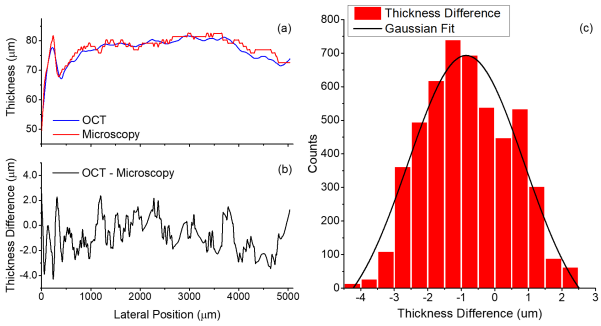

FIGURE 7. (a) The CC thickness measured by microscope (red curve) and OCT (blue curve), respectively; (b) The CC thickness difference (OCT - Microscope), with averaged difference of −0.82 μm and standard deviation of 1.30 μm; (c) Histogram of the thickness difference distribution, and Gaussian fit yields a FWHM of 4.06 μm.

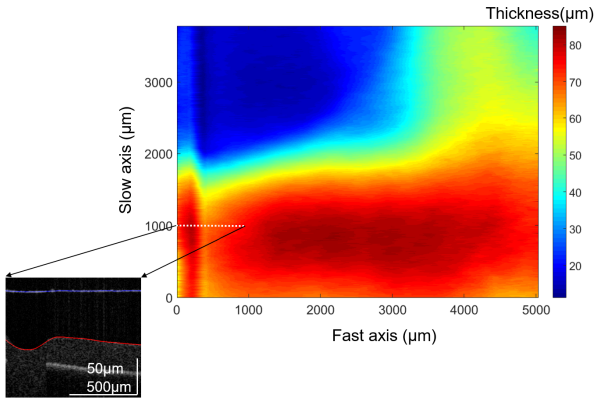

FIGURE 8. Thickness map of the conformal coating covering an area about 5.03mm × 3.77mm. The OCT cross-section image on the lower-left corner corresponds to the region delineated by the white dashed line in the thickness map.

Fig. 7(b), the black curve is the Gaussian fit on the histogram of the thickness difference with a FWHM of 4.06 μm.

This difference can be partly attributed to the limited resolutions of OCT system (1.72 μm in air) and microscopy (1 μm for the objective-PlanApo D 5 × /0.3, Zeiss, Oberkochen, GER). In addition, the coating measurement algorithm for OCT image and manual measurement for microscopic image can also come with a limited accuracy. These two facts above imply that the difference of about 4 μm between these two methods is reasonably acceptable. Overall, the results demonstrated that ultra-high resolution OCT can provide accurate thickness measurements for the conformal coating on PCB and has the potential to replace the conventional method.

Furthermore, a thickness map was generated by utilizing the three-dimensional imaging capability of OCT. The results are illustrated in Fig. 8. With the color coding on the thickness, it is easy to catch the thickness variation. For example, there is a sharp thickness change along the white dashed line in the thickness map, which is consistent with the finding shown in the OCT cross-sectional image on the lower-left corner in Fig. 8. In comparison, the thickness map is very hard to be obtained for the conventional microscopy method because the PCB needs to be processed and cross-sectioned for the thickness measurement. Moreover, the region of interest is selected randomly for the thickness measurement and consequently, it unavoidably takes the risk of missing the problematic coating region. In addition, the thickness measurement on the image acquired under a microscope is usually performed manually. This may lead to an inter-operator variation and slow down the measurement speed compared to our measurement algorithm. All the discussions above indicates that OCT technique allows for a quick mass inspection of the entire coating region on the PCB while this is difficult for the conventional method. Although, from the measurement accuracy point of view, the microscopy method can improve its accuracy by using high numerical aperture objective while this is more difficult for OCT method, however, it suffers from a decrease in field of view and consequently a lower measurement speed. Overall, it can be fairly concluded that OCT has a great potential to replace the conventional microscopy for the thickness measurement of the conformal coating on the PCBs.

IV. CONCLUSIONS

In this study, we explored the feasibility of ultra-high resolution SD-OCT for the conformal coating thickness measurement. A flexible and robust SD-OCT system was developed with a low-cost and an axial resolution of $\sim$ 1.72 μm. The system cost was mainly due to a low-cost supercontinuum light source ($\sim$10,000 USD) and CCD detector ($\sim$4000 USD, this can be further reduced in the future). High-quality images of the conformal coating can be obtained, and an image segmentation algorithm was also designed to detect and measure the thickness of the conformal coating layer from the high-quality OCT images. The measurement results are highly consistent with those by the conventional method, indicating a good efficacy of high resolution OCT in the conformal coating thickness measurement. Compared to the conventional method, the thickness measurement with OCT is rapid and non-destructive, demonstrating that OCT has a good potential to be used for online monitoring of the conformal coating thickness in PCB assembly line. In addition to the thickness inspection, SD-OCT can also be useful to detect and map the localized defects in the PCB conformal coating, which thus helps optimize the coating process.

ACKNOWLEDGMENT

The authors would thank Yuhui Ma for the helpful discussions and advices about the segmentation algorithm. *(Xiao Shao and Xinjian Chen are co-first authors.)*

REFERENCES

[1] K. Zhang and M. Pecht, "Effectiveness of conformal coatings on a PBGA subjected to unbiased high humidity, high temperature tests," *Microelectron. Int.*, vol. 17, no. 3, pp. 16–20, 2000.

[2] S. Zhan, M. H. Azarian, and M. G. Pecht, "Surface insulation resistance of conformally coated printed circuit boards processed with no-clean flux," *IEEE Trans. Electron. Packag. Manuf.*, vol. 29, no. 3, pp. 217–223, Jul. 2006.

[3] S. Han, M. Osterman, S. Meschter, and M. Pecht, "Evaluation of effectiveness of conformal coatings as tin whisker mitigation," *J. Electron. Mater.*, vol. 41, no. 9, pp. 2508–2518, 2012.

[4] M. Osterman, "Effectiveness of conformal coat to prevent corrosion of nickel-palladium-gold-finished terminals," in *Proc. IPC APEX EXPO*, 2014, pp. 1–8.

[5] I. B. Goldman and A. Krajewski, "Conformal coating thickness determination: A comparison of methods," in *Proc. EIC 6th IEEE Elect./Electron. Insul. Conf.*, Oct. 1983, pp. 288–294.

[6] C. Petrilli, "The basics of coating thickness measurement," *Metal Finishing*, vol. 99, no. 8, pp. 8–13, 2001.

[7] D. Huang *et al.*, "Optical coherence tomography," *Science*, vol. 254, no. 5035, pp. 1178–1181, 1991.

[8] M. R. Hee *et al.*, "Optical coherence tomography of the human retina," *Arch. Ophthalmol.*, vol. 113, no. 3, pp. 325–332, 1995.

[9] J. Welzel, "Optical coherence tomography in dermatology: A review," *Skin Res. Technol.*, vol. 7, no. 1, pp. 1–9, 2001.

[10] M. D. Radu, "The contribution of optical coherence tomography to interventional cardiology," Erasmus Univ. Rotterdam, Rotterdam, The Netherlands, Tech. Rep., 2014.

[11] T. Tsung-Han, J. G. Fujimoto, and M. Hiroshi, "Endoscopic optical coherence tomography for clinical gastroenterology," *Diagnostics*, vol. 4, no. 2, pp. 57–93, 2014.

[12] Y. Dong, S. Lawman, Y. Zheng, D. Williams, J. Zhang, and Y. C. Shen, "Nondestructive analysis of automotive paints with spectral domain optical coherence tomography," *Appl. Opt.*, vol. 55, no. 13, pp. 3695–3700, 2016.

[13] G. Hannesschläger *et al.*, "Optical coherence tomography as a tool for non destructive quality control of multi-layered foils," in *Proc. 6th NDT Prog.*, 2011, pp. 9–10.

[14] M. Sabuncu and M. Akdoğan, "Utilizing optical coherence tomography in the nondestructive and noncontact measurement of egg shell thickness," *Sci. World J.*, vol. 2014, no. 4, 2014, Art. no. 205191.

[15] S. Lawman and H. Liang, "High precision dynamic multi-interface profilometry with optical coherence tomography," *Appl. Opt.*, vol. 50, no. 32, pp. 6039–6048, 2011.

[16] A. Nemeth, G. Hannesschläger, E. Leiss-Holzinger, K. Wiesauer, and M. Leitner, "Optical coherence tomography–applications in nondestructive testing and evaluation," in *Optical Coherence Tomography*. Rijeka, Croatia: InTech, 2013.

[17] S. Chang, Y. Mao, G. Chang, and C. Flueraru, "Jade detection and analysis based on optical coherence tomography images," *Opt. Eng.*, vol. 49, no. 6, 2010, Art. no. 063602.

[18] R. Su, M. Kirillin, E. W. Chang, E. Sergeeva, S. H. Yun, and L. Mattsson, "Perspectives of mid-infrared optical coherence tomography for inspection and micrometrology of industrial ceramics," *Opt. Express*, vol. 22, no. 13, pp. 15804–15819, 2014.

[19] K. A. Serrels, M. K. Renner, and D. T. Reid, "Optical coherence tomography for non-destructive investigation of silicon integrated-circuits," *Microelectron. Eng.*, vol. 87, no. 9, pp. 1785–1791, 2010.

[20] N. H. Cho, U. Jung, S. Kim, and J. Kim, "Non-destructive inspection methods for leds using real-time displaying optical coherence tomography," *Sensors*, vol. 12, no. 8, pp. 10395–10406, 2012.

[21] J. Czajkowski, T. Prykäri, E. Alarousu, J. Palosaari, and R. Myllylä, "Optical coherence tomography as a method of quality inspection for printed electronics products," *Opt. Rev.*, vol. 17, no. 3, pp. 257–262, 2010.

[22] J. Czajkowski *et al.*, "Ultra-high resolution optical coherence tomography for encapsulation quality inspection," *Appl. Phys. B, Lasers Opt.*, vol. 105, no. 3, pp. 649–657, 2011.

[23] X. Yu, X. Liu, S. Chen, Y. Luo, X. Wang, and L. Liu, "High-resolution extended source optical coherence tomography," *Opt. Express*, vol. 23, no. 20, pp. 26399–26413, 2015.

[24] G. J. Tearney, M. E. Brezinski, J. F. Southern, B. E. Bouma, M. R. Hee, and J. G. Fujimoto, "Determination of the refractive index of highly scattering human tissue by optical coherence tomography," *Opt. Lett.*, vol. 20, no. 21, pp. 2258–2260, 1995.

XIAO SHAO received the bachelor's degree in electrical information engineering from the Changshu Institute of Technology, in 2011. He is currently a Graduate Student at Soochow University, Suzhou, China. His current research is focused on optical coherence tomography and optical coherence elastography.

XINJIAN CHEN received the Ph.D. degree from the Chinese Academy of Sciences, in 2006. He is currently a Distinguished Professor with Soochow University, Suzhou, China. He conducted postdoctoral research at the University of Pennsylvania, the National Institute of Health, and the University of Iowa, USA, from 2008 to 2012. He has published over 150 international journals and conference papers. He holds 14 patents.

XIAOJUN YU received the Ph.D. degree from Nanyang Technological University, Singapore, in 2015, where he was a Postdoctoral Research Fellow, from 2015 to 2017. He is currently an Associate Professor with Northwestern Polytechnical University, China. His main research interests include high-resolution optical coherence tomography and its imaging applications.

YA HU received the bachelor's degree in mechanical engineering and the master's degree in electrical engineering from Soochow University, in 2016. In 2011, he started his working career at Bosch Engineering. From 2011 to 2014, he worked on testing and failure analysis in electrical control unit and then continued his work on system reliability for hardware development. He is currently a Senior Hardware Project Management Engineer with Bosch Automotive Products (Suzhou) Co., Ltd. He also works on the project management of hardware development. He is also a Professional in electrical development, production, and industry.

LINBO LIU received the B.Eng. degree in precision instrument and the M.Eng. degree in optical engineering from Tianjin University, China, in 2001 and 2004, respectively, and the Ph.D. degree in bioengineering from the National University of Singapore, in 2008. He did his Postdoctoral Training at the Wellman Center for Photomedicine, Harvard Medical School (HMS), Massachusetts General Hospital, from 2008 to 2011. He was promoted as an Instructor of dermatology at HMS. He has been the Nanyang Assistant Professor with the School of Electrical and Electronic Engineering and the School of Chemical and Biomedical Engineering, since 2012. His research interests include the development and validation of non-invasive, cellular, and sub-cellular resolution imaging methods for disease diagnosis and life science research.

FEI SHI received the Ph.D. degree in electrical engineering from Polytechnic University, USA, in 2006. She is currently an Assistant Professor with Soochow University, Suzhou, China. She has co-authored over 40 papers in internationally recognized journals and conferences. Her current research interests include medical image processing and analysis.

WEI SHAO received the master's degree in electrical and computer engineering from the University of Iowa, USA, in 2016, where he is currently pursuing the Ph.D. degree. His research interests include the field of medical imaging and computational anatomy.

JIANHUA MO received the B.Eng. degree in information instrument and the M.Eng. degree in optical engineering from Zhejiang University, China, and the Ph.D. degree in biomedical engineering from the National University of Singapore, in 2011. He did his Postdoctoral Training in VU University Amsterdam before joining Soochow University, Suzhou, China, in 2014. He is currently an Associate Professor with Soochow University. His research interests include the optical imaging and spectroscopy techniques for biomedical applications and non-destructive inspection in industry.